INTERFACE SCIENCE 11, 439–450, 2003

Stimulation and Suppression of Grain Boundary Sliding by Intragranular Slip in Zinc Bicrystals

A.D. SHEIKH-ALI*,† AND J.A. SZPUNAR
Department of Mining, Metals and Materials Engineering, McGill University, 3610 University Street, Montreal, Quebec, H3A 2B2, Canada
sheikh@magnet.fsu.edu

H. GARMESTANI
FAMU-FSU College of Engineering, Tallahassee, FL 32310, USA

Abstract. The influence of intragranular slip on grain boundary sliding is studied in originally compatible zinc bicrystals with symmetric tilt boundary. The experiment is designed to separate different effects of intragranular slip on the boundary sliding and establish their mechanisms. Grain boundary sliding with and without development of intragranular slip is observed. The rate of sliding accompanied by slip is more than five times of that without slip. A good correlation between the boundary sliding and intragranular slip prior to slide hardening is established. Slide hardening followed by the negative sliding near one end of the boundary and strain hardening in the boundary vicinity, are observed at the last stages of deformation. For the case of formation of slip induced glissile grain boundary dislocations of opposite signs the possibility of their contribution to total grain boundary sliding, is analyzed. The effect of the increase in the rate of sliding is explained in terms of the accommodation of sliding by slip and appearance of additional glissile grain boundary dislocations of one sign due to strain incompatibility. Contribution of these different dislocation mechanisms to the increase in the sliding rate is determined for the stage of deformation preceding slide hardening. It is supposed that the effect of slide hardening and negative sliding as well as boundary curving is created by non-smooth boundary and small degree of incompatibility caused by straining.

Keywords: grain boundary sliding, intragranular slip, grain boundary dislocation, zinc bicrystal

1. Introduction

Grain boundary sliding (GBS) is an important mode of deformation of polycrystalline materials. At high temperatures its contribution to the overall strain can be extremely high. Grain boundary sliding is often accompanied by intragranular (crystallographic) slip. Usually, the interaction of intragranular slip with boundary enhances the rate of grain boundary sliding [1–4]. It has been demonstrated in zinc and cadmium bicrystals of special geometry that the rate of grain boundary sliding in the presence of intragranular slip can be higher than grain boundary sliding in the absence of intragranular slip by more than an order of magnitude ("pure" GBS) [2, 3]. In addition, for the same type of bicrystals it has been demonstrated that the rate of intragranular strain is in a good correlation with the rate of GBS [4]. Basically, different mechanisms can be responsible for the increase in the rate of GBS: accommodation of grain boundary sliding by slip at grain boundary irregularities [5], achievement of non-equilibrium [6] or high-excited [7] boundary states due to interaction

*To whom all correspondence should be addressed.
†On leave from the Institute for Metals Superplasticity, Russian Academy of Sciences, Ufa, Russia. Now at FSU-National High Magnetic Field Laboratory and FAMU-FSU College of Engineering, 1800 East Paul Dirac Drive, Tallahassee, FL 32310, USA.

with lattice dislocations, participation of slip of lattice or slip induced grain boundary dislocations (GBDs) in GBS [8–17]. Theory of boundary transition into high-excited state with a small resistance to sliding [7] has not been proved and has contradictions with existing experimental results on sliding. The non-equilibrium state of grain boundary is characterized by long-range elastic fields due to irregular arrangements of sessile GBDs and/or by the presence of glissile grain boundary dislocations of one sign [18]. Motion of sessile GBDs does not make any contribution to sliding. Glissile GBDs of one sign are induced by incompatible deformation and can directly contribute to the sliding. It has been shown that the effect of stimulation of sliding by slip is observed during deformation of originally compatible bicrystals [4]. Also, it has been shown that at compatible deformation (identical deformation of grains with respect to their common boundary) there is no contribution of slip-induced glissile GBDs of opposite signs to the sliding [19]. However, compatibility conditions change during straining and dislocation reactions producing residual glissile GBDs of one sign can be activated. Therefore, it remains unclear whether the stimulation effect occurs at compatible deformation or the main reason for it is a small incompatibility appearing with the change in bicrystal geometry. The aim of this investigation is to study the influence of intragranular slip on GBS in originally compatible zinc bicrystals whose deformation results in the appearance of small degree of plastic strain incompatibility and separate the effects of intragranular slip on sliding at compatible and incompatible stages of deformation.

2. Design of Bicrystal Experiments

Zinc bicrystal with geometry and schematic of deformation shown in Fig. 1 can be considered as plastically compatible according to the definition of Chalmers and coworkers [20, 21]. Bicrystal contains symmetric tilt $90^\circ\langle 10\bar{1}0\rangle$ boundary tilted at an angle of 60° with respect to the tensile axis (Fig. 1(a)). All other angles of boundary inclination except 30° and 90° cannot provide compatibility conditions of deformation for given boundary misorientation. The directions of shear stresses and signs of edge LDs gliding over basal planes under the applied stresses are predetermined by given loading conditions (Fig. 1(b)). Although basal planes in neighboring grains have different inclination angles with respect to the deformation axis the Schmid factors for basal slip are the same in both grains. Therefore, in the initial stage of deformation shears in the grains are the same and grains deform similarly in the boundary plane. In other words, this bicrystal completely meets conditions for compatible deformation [20, 21]:

$$\varepsilon^A_{XX} \neq \varepsilon^B_{XX}, \quad \varepsilon^A_{ZZ} = \varepsilon^B_{ZZ}, \quad \varepsilon^A_{XZ} = \varepsilon^B_{XZ} = 0 \qquad (1)$$

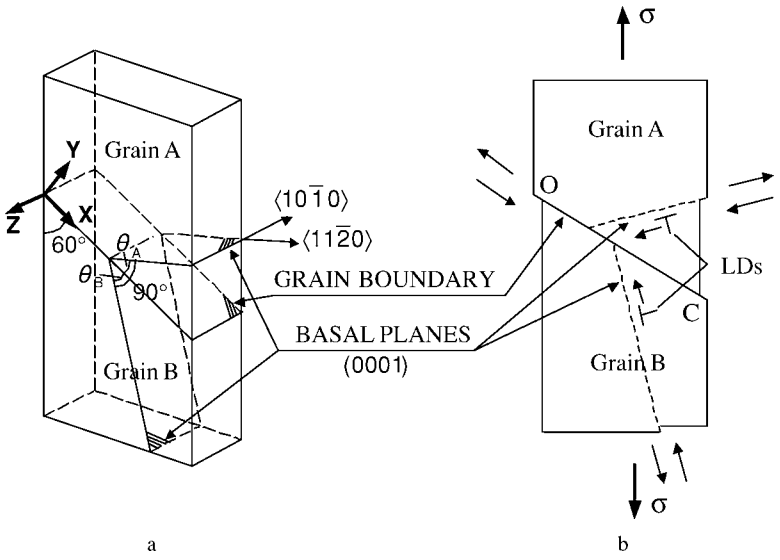

Figure 1. Crystallography of specimen (a) and geometry of intragranular slip and sliding (b). Double arrows indicate the directions of shear stresses along the basal planes and the boundary.

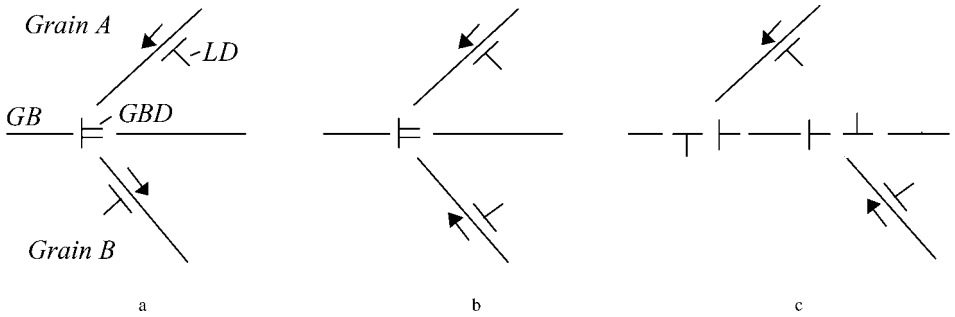

Figure 2. Formation of residual grain boundary dislocations as a result of dislocation reactions during compatible deformation.

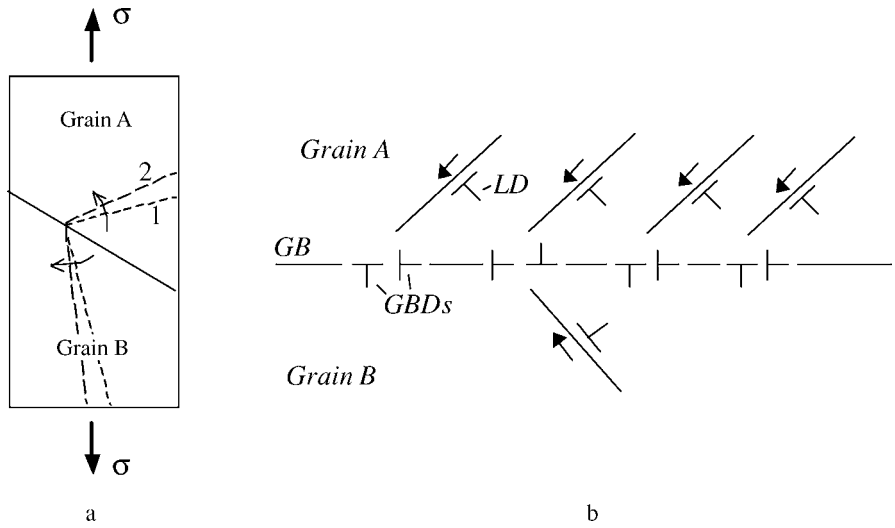

Figure 3. Rotation of basal slip planes during tension of bicrystal, which increases the difference between shear stresses in different grains (a) and results in generation of glissile GBDs of predominantly one sign (b).

Due to the absence of strain in Z direction the deformation of bicrystal can be considered as two-dimensional (Fig. 1(b)). At micro-level dislocation reactions produce residual sessile GBDs as a result of transmission of lattice dislocations through the boundary (Fig. 2(a)) or meeting of lattice dislocations at the same point of the boundary (Fig. 2(b)). In spite of strain compatibility at macro-level there is a high probability of dilatational mismatch along the boundary at micro-level or micro-incompatibility [22]. If lattice dislocations from different grains enter the boundary at different points their dissociation produces glissile GBDs with opposite signs (Fig. 2(c)).

Straining of bicrystal results in the appearance of some degree of incompatibility. Due to crystallographic rotation of grains Schmid factor for basal slip in Grain A increases and in Grain B decreases (Fig. 3(a)) which results in the loss of similarity of strain in grains:

$$\varepsilon_{XX}^{A} \neq \varepsilon_{XX}^{B}, \quad \varepsilon_{ZZ}^{A} = \varepsilon_{ZZ}^{B}, \quad \varepsilon_{XZ}^{A} = \varepsilon_{XZ}^{B} = 0 \qquad (2)$$

Therefore, following Hauser and Chalmers [20], this type of bicrystal can be related to transiently compatible bicrystals whose compatibility can be provided only at the initial stage of deformation. Plastic incompatibility due to enhanced deformation of Grain A creates additional number of glissile GBDs of the same sign (Fig. 3(b)).

3. Experimental Details

Zinc bicrystals (99.97%) containing a $88.7^\circ \pm 0.5^\circ$ $\langle 10\bar{1}0 \rangle$ symmetrical tilt boundary was used (Fig. 1).

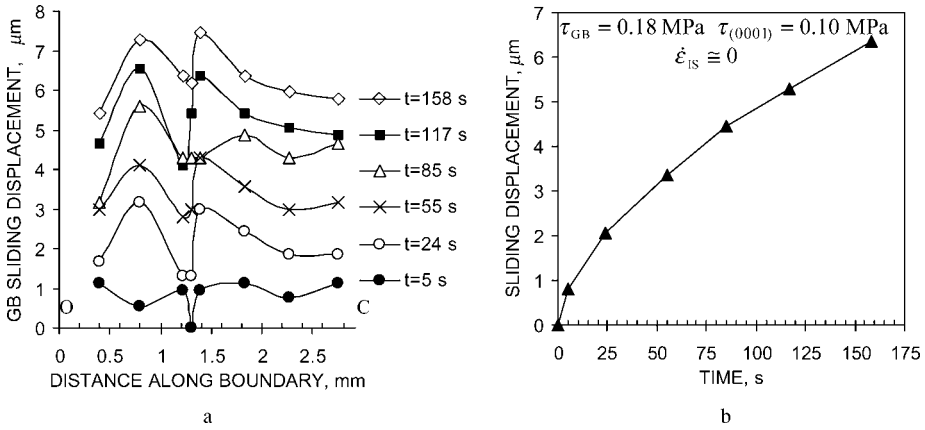

Figure 4. Non-uniformity of sliding along the boundary and average sliding rate as a function of testing time for bicrystal deformed at $\sigma =$ 0.42 MPa.

A bicrystalline plate was grown from the melt in a horizontal graphite boat by the Bridgman method in an argon atmosphere. Specimens were spark cut from a bicrystal plate at 60° with respect to the boundary line. The geometry of slip in this type of bicrystal is considered in the previous section. Dimension of bicrystalline specimens were $25 \times 3.5 \times 2$ mm^3. The damaged layer adjacent to the surfaces was removed by chemical polishing on the acid-resistant cloth. Final polishing was performed electrolytically. On the polished bicrystal surfaces, the families of marker lines to be used for measuring GBS and IS were scratched by a diamond tip. Both lines parallel to the tensile direction (longitudinal scratches) and parallel to the boundary were made. The magnitudes of GBS were determined by the shift of longitudinal scratches. The average value of intragranular strain was determined by elongation of segments on the longitudinal scratches. These segments are formed by intersection of longitudinal scratches with scratches parallel to the boundary. The average length of the segments was around 100 μm. Bicrystals were tensile strained at constant load at 553 K (0.8 T_{melt}). Tests were performed at two values of initial stress: $\sigma = 0.42$ and 0.44 MPa which corresponded to the values of shear stress along the boundary: $\tau = 0.18$ and $\tau = 0.19$ MPa, respectively. Shear stresses along the basal planes were $\tau = 0.10$ and $\tau = 0.11$ MPa. To exclude bending stresses, deformation was carried out using independent and freely movable grips that could provide the rotational movement of the ends of bicrystalline specimens.

4. Results

Grain boundary sliding at smaller stress ($\sigma =$ 0.42 MPa) is not accompanied by a noticeable boundary migration and intragranular slip. No slip lines can be observed in the vicinity of the boundary in both grains. Figure 4 illustrates the distribution of grain boundary sliding along the boundary (Fig. 4(a)) and its average amount versus testing time (Fig. 4(b)). The amounts of sliding oscillation remain almost the same for the majority of the boundary points during the whole deformation (Fig. 4(a)). The sliding rate decreases with time (Fig. 4(b)). Direct measurement of intragranular slip using marker lines does not reveal any strain near the boundary during the whole test. Grain boundary sliding at higher stress ($\sigma = 0.44$ MPa) is accompanied by irregular boundary migration. Also, slip lines ending at or transmitting across the boundary are observed (Fig. 5(a)). Macroscopically the shape of bicrystal changes and the boundary becomes curved as a result of deformation gradient (Fig. 5(b)). Figure 6 displays GBS versus distance along the boundary for different testing time. It shows that sliding is distributed non-uniformly along the boundary and there is some trend of its increase from one end of the boundary to the other at the last stages of deformation. Figure 7 shows grain boundary sliding measured near points O and C as a function of time. The dependence of GBS versus time looks complex. With straining the rate of sliding is increasing, decreasing, changing sign and stagnating. Figure 7 also contains intragranular strain versus time curve for both grains of bicrystal. The rate of

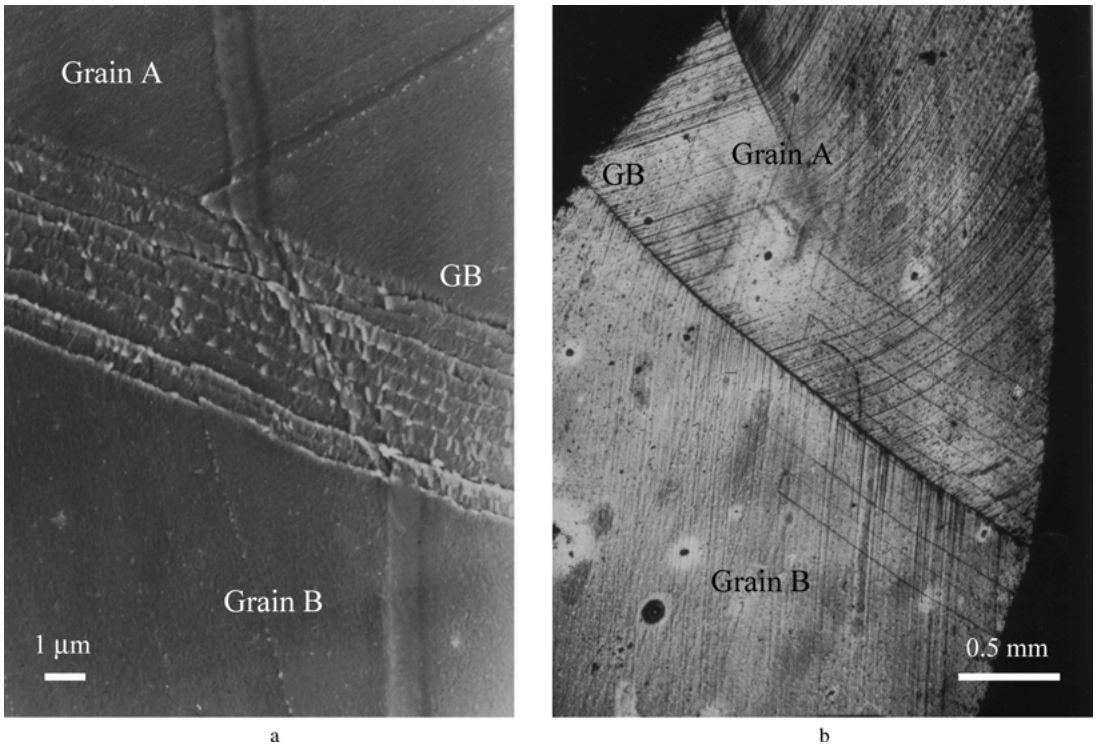

Figure 5. Scanning electron (a) and optical (b) micrographs of deformed bicrystal.

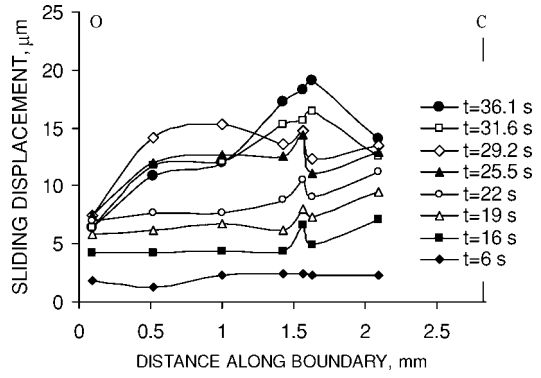

Figure 6. Variations of the amount of sliding along the boundary after different testing time.

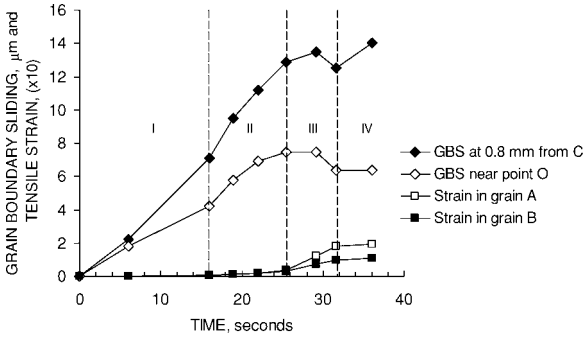

Figure 7. Variations of intragranular shears along the boundary in grains *A* (a) and *B* (b) after different testing time.

intragranular slip measured near the boundary changes with straining. There is a pronounced correlation between sliding and strain during first 25 s of deformation. After this period the decrease in the sliding rate up to zero followed by the change in the direction of sliding corresponds to sharp increase in the rate of slip and the appearance of a marked difference of strain in grains. The decreased rate of intragranular slip at the end of deformation corresponds to the stagnation of sliding. Figure 8 shows distribution of intragranular shear along the boundary in grains *A* and *B*. It is seen that there is no much difference between shears in different grains near the same place of the boundary. Shear in grain *A* is slightly higher than that in grain *B*. Figure 9 shows the change of different parameters of bicrystal calculated from intragranular strain using well-known relationships between strain, shear and its

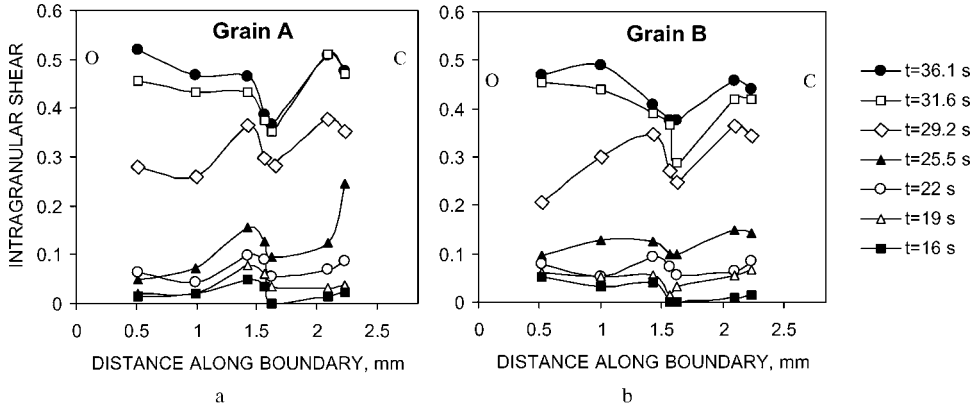

Figure 8. Grain boundary sliding and shear strain as functions of time for bicrystal strained at $\sigma = 0.44$ MPa and $T = 553$ K.

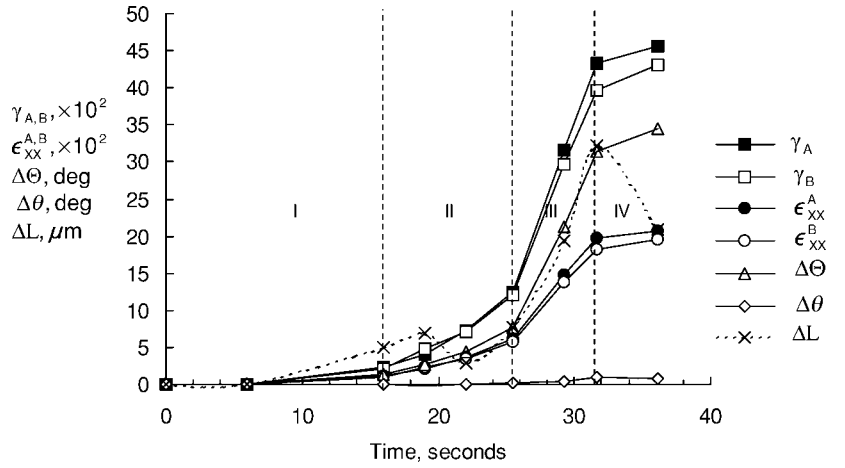

Figure 9. Different parameters of bicrystal calculated from intragranular strain as functions of time (explanation in the text).

orientation to the tensile axis [23]. They include shear along basal planes in both grains γ_A and γ_B, strains in the boundary plane ε^A_{XX} and ε^B_{XX}, angle of deviation from original misorientation $\Delta\Theta$, angle of deviation of boundary plane from its symmetry position $\Delta\theta$ that can be determined as $\Delta\theta = (\theta_A - \theta_B)/2$ and difference between fiducial boundary segments in grains A and B $\Delta L = L_B - L_A$. At the beginning of the test that segments have the same length of 2 mm. It is seen that the difference in intragranular shears and in strains at boundary plane becomes marked after 25 s of testing. The angle of deviation from original boundary misorientation $\Delta\Theta$ reaches 7.6° at 25 s of test and ~35° at the end of the test. Thus, at the end of the test the boundary misorientation increases up to ~125°. Remarkably, the boundary retains a high degree of symmetry, the maximum angle of deviation from symmetry reached at the end of deformation is only ~1°. The difference between fiducial segments ΔL characterizes sliding induced by plastic strain incompatibility, which increases with straining. The maximum difference of $\Delta L = 30$ μm is achieved at 32 s of test. Figure 10 shows the average amount of GBS as a function of time for specimens with and without macroscopic intragranular strain in grains. The small difference in shear stress along the boundary for different samples allows us to compare sliding rates in both cases. The rate of GBS when it is accompanied by intragranular deformation can be more than five times of the sliding rate without intragranular deformation.

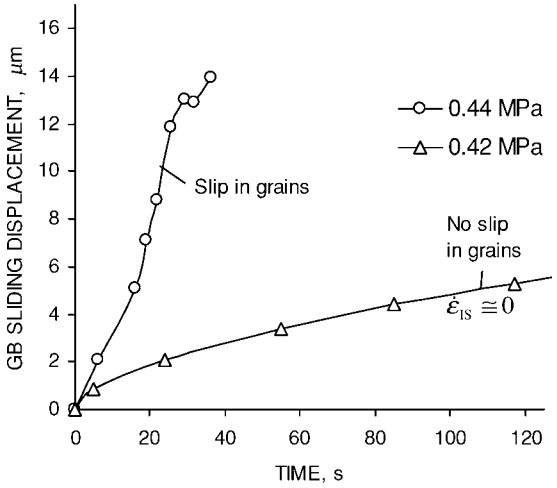

Figure 10. Amount of grain boundary sliding versus time for two bicrystals tested at slightly different stresses. The two curves correspond to cases where intragranular slip either occurs, or does not occur, while the sliding takes place.

5. Discussion

5.1. Relation Between Intragranular Slip and Grain Boundary Sliding

The deformation of bicrystal at smaller stress is sufficient to activate GBS and is not enough to induce intragranular slip. The main difference of this type of sliding from pure GBS observed in zinc bicrystals which geometry excludes the appearance of applied shear stresses along basal planes [2] is the possibility of accommodation of sliding by the emission of lattice dislocations from the boundary irregularities. Superposition of applied and local stresses at boundary irregularities might result in the emission of a few lattice dislocations from each boundary source, which, however, escapes revealing due to insufficient resolution of optical microscopy.

Deformation of bicrystal at higher stress results in coexistence of both: GBS and marked intragranular deformation. A good correlation between slip and sliding during first 25 seconds of bicrystal deformation in this case can be explained by the effect of stimulation of GBS by crystallographic slip. Sigmoid type of GBS and strain versus time curves observed in our case (Fig. 7) are not uncommon for the creep of single crystals at low stresses and is likely to be associated with inhomogeneous deformation [24]. Usually, spatial macroscopic non-uniformity of GBS is a result of difference in strain in neighboring grains or plastic strain incompatibility [25, 26]. Figure 6 shows a large non-uniformity of GBS observed at the last stages of bicrystal deformation that reaches 13 μm at the distance of 2 mm. Figure 7 shows strain and geometrical parameters of bicrystal versus time. The difference in fiducial boundary segments in grain A and $B\Delta L$ which is calculated from strains in the vicinity of the boundary achieves 30 μm. A significant difference between directly measured and calculated values of ΔL can be explained by a significant strain gradient in the normal direction Y within measured segments. The existence of strain gradients is seen from curved slip lines in Fig. 5(b). A large strain gradient is a cause of kinking in Grain A. Not all dislocations providing intragranular deformation in the boundary region enter the boundary. The inefficiency of grain boundary recovery processes can be explained by the existence of boundary irregularities or boundary micro-roughness. Despite of short running distance, glissile GBDs produced from lattice dislocations forms pile-ups near steps and/or facets, which creates long-range elastic fields [26]. The strain gradient normal to the boundary also results in boundary macro-convexity oriented to the grain B (Fig. 5(b)). In the absence of GBS the curvature of the boundary depends only on difference of strains in grains. However, even in the case of ideal smooth boundary able to slide perfectly the radius of curvature cannot be expected as equal to infinity. Gradient of strain seems to be also responsible for grain boundary migration. It is seen from the alternation of GBS and the boundary migration. Such boundary behavior is not inherent to vicinal boundaries [27]. Therefore, glissile GBDs participating in GBS cannot be considered as DSC-dislocations. In other words, this boundary does not consist of one sort of structural unit as one of the requirements for the existence of a special boundary [28] or the number of major structural units is insufficiently high in comparison with the number of minor structural units that belong to the neighboring favored boundary. Since the boundary is supposed to be general or non-favored one, the glissile GBDs have infinitesimal Burgers vectors [29] of two opposite orientations parallel to the boundary line. Although the value of the Burgers vector of these dislocations is uncertain the description of GBS in terms of motion of glissile GBDs looks more realistic than sliding by simultaneous shear along the entire boundary. Strain hardening near the boundary and slide hardening observed at the last stages of deformation can both have the same origin. Incompatible deformation results

in generation of slip induced sliding due to generation of GBDs of one sign. If they move in one direction, slip induced sliding fully contributes to the overall sliding [30]. In this case, sliding produced by GBDs generated at grain boundary sources is determined by sliding near point O. Sliding near this point is also sensitive to the motion of GBDs in opposite direction at high intragranular slip rates [31]. The possible reasons for the lost of correlation can be slide hardening and generation of slip induced sliding which cannot contribute entirely to overall elongation of bicrystal. Formation of GBD pile-ups near grain boundary irregularities (steps and facets) creates back stresses which result in the motion of part of GBDs contrary to the applied stresses. This process continues till intragranular slip decreases drastically. At the last stage of straining this effect exceeds stimulating effect of intragranular slip on GBS. Thus, intragranular slip can both stimulate and suppress sliding. Small difference in stresses applied to bicrystals allows us to compare the rates of sliding in the presence and in the absence of intragranular slip. It is seen from Fig. 10 the rate of stimulated GBS can be more than five times of that for pure sliding. The possible mechanisms of this effect are considered below.

5.2. *Mechanism of Stimulation of Sliding by Slip During Compatible Deformation*

The interaction between lattice dislocations and grain boundary at high temperatures often results in generation of glissile component of grain boundary dislocation even at compatible deformation. At high temperatures transmission of lattice dislocation through the boundary that produces sessile GBD is a quite rare event because it is substituted by the process of dissociation of lattice dislocation impinged into the boundary [32]. The probability of the meeting of lattice dislocations at the same point of the boundary seems to be extremely low. Therefore, in some models [3, 11, 33] the effect of stimulation of grain boundary sliding by intragranular slip during compatible deformation is still ascribed to the appearance of additional density of mobile GBDs contributing to the sliding. For example, recently proposed model of GBS [33] based on geometry of zinc and cadmium bicrystals [2, 3] considers two families of glissile GBDs of opposite signs produced from the interaction of lattice dislocations with the boundary. According to this model, namely these additional GBDs are responsible for increase in the rate of sliding. Unfortunately, this model makes no difference between dislocations generated by grain boundary sources and induced by intragranular slip. Further we analyze the contribution slip induced GBDs of opposite signs to grain boundary sliding.

Let us consider the interaction of lattice dislocations of different grains with the boundary during compatible deformation. We can assume that lattice dislocations are impinging into different equal-spaced points in the boundary (Fig. 11(a)). Lattice dislocations originated from Grain A appear in the boundary points designated as A_n, $A_{n+1}, \ldots, A_{n+i}$. Analogously, for the lattice dislocations that enter the boundary from Grain B the boundary points are designated as B_n, $B_{n+1}, \ldots, B_{n+i}$. For simplicity we assume that the number of dislocations coming to each point are the same and these dislocations appear simultaneously. Also, we assume that this hypothetical bicrystal contains microscopic flat boundary and that GBDs are not generated by grain boundary dislocation sources during GBS. Lattice dislocations entering the boundary dissociate into glissile and sessile GBDs. Motion of glissile GBDs under the applied stresses occurs in opposite directions and therefore, results in their mutual annihilation. However, these GBDs move and produce GBS only within some boundary segments which can be designated as A_nB_n, $A_{n+1}B_{n+1}, \ldots, A_{n+i}B_{n+i}$.

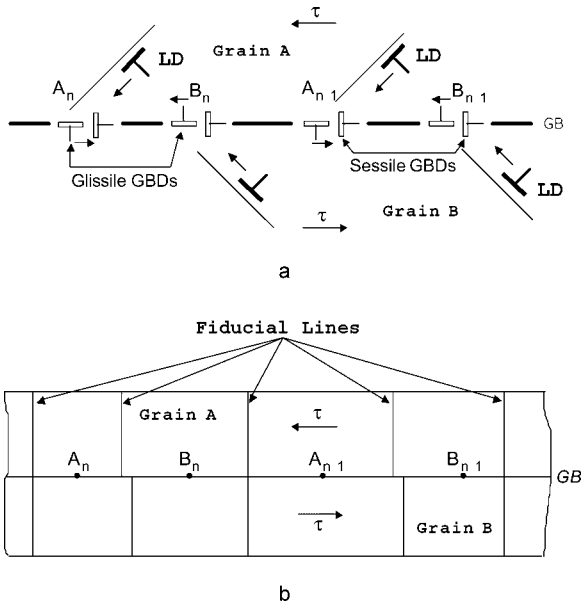

Figure 11. Formation of GBDs as a result of lattice dislocations entering the boundary (a). Portion of the bicrystal after deformation, illustrating boundary segments with and without displacement of fiducial lines (b).

There is no movement of GBDs along boundary segments $B_nA_{n+1}, B_{n+1}A_{n+2}, \ldots, B_{n+i-1}A_{n+i}$ and hence, no sliding within these segments. If fiducial lines are scratched on the bicrystal surface across each boundary segment before the deformation, we can see alternation of segments with and without displacement of these lines after the deformation (Fig. 11(b)). When the amount of sliding reaches the length of segment, the shifted fiducial lines stops at the ends of these segments; although GBS along the segments can be in progress. Coexistence of these two different kinds of segments indicates that there is no continuous shear of one crystal in respect to the other. Therefore, this type of GBS cannot make a direct contribution to total deformation because it does not produce continuous shift of one crystal with respect to the other along the whole boundary. For this reason, local GBS can be considered only as one of the processes of grain boundary recovery that removes micro-incompatibility and facilitates intragranular deformation. If we assume that GBDs are generated by grain boundary dislocation sources under the applied stresses and induce the sliding which makes a direct contribution to total deformation, the superposition of local GBS does not increase this contribution. It is worth to note that in the case when all slip lines have common points at the boundary the continuous sliding may occur. However, for the continuous sliding the processes of entry of lattice dislocations into the boundary, their dissociation and motion of GBDs should be mutually coordinated along the whole boundary to avoid interaction between dislocations entering the same points from different grains (Figs. 12(a) and (b)). Such self-organization of deformation is energetically unfavorable. Moreover, in most cases, the common points of slip lines is a result of transmission of lattice dislocations through grain boundary [32]. Since the boundary is symmetric, only sessile GBDs should appear at transmission of dislocations through the boundary. Therefore, the probability of transformation of local GBS to continuous one is extremely low. Thus, in the case of plastic strain compatibility the GBDs originated from lattice dislocations impinged into the boundary cannot increase the rate of macroscopic GBS. A stimulation effect of crystallographic slip on sliding observed on bicrystals [2, 3], can be understood if we assume that grain boundary contains a microscopic irregularities such as, for example, steps as shown in Fig. 13. These barriers can be overcome if a part of GBDs are involved in the reactions of generation of lattice dislocations with their subsequent emission to the grain

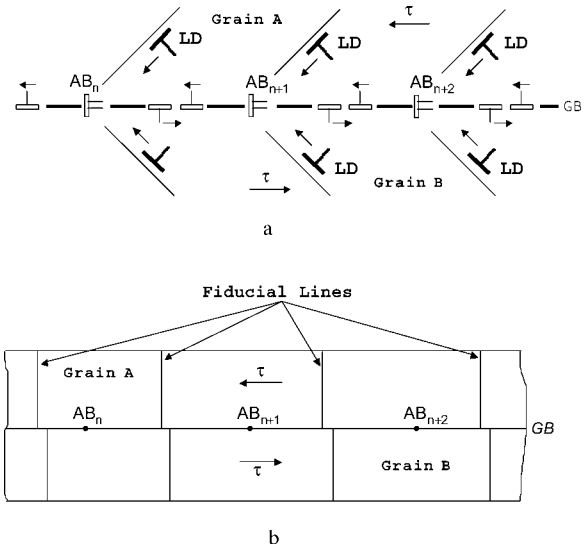

Figure 12. Mutually coordinated dislocation reactions in the boundary. Appearance of glissile GBDs of opposite signs from lattice dislocations of different grains entered the same points of the boundary (a). Portion of bicrystal showing displacement of fiducial lines in different boundary segments (b).

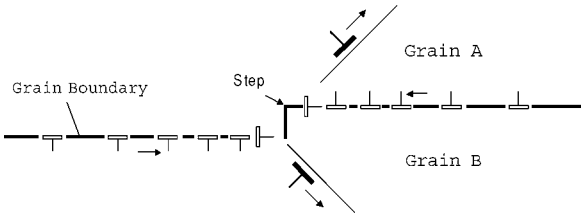

Figure 13. Generation of lattice dislocations from boundary steps during the sliding along $90^\circ\langle 10\bar{1}0\rangle$ boundary.

interior. For given compatibility conditions, dislocation mechanism of accommodation of sliding seems to be quite realistic. It is worth to note that exact mechanism of accommodation of sliding by intragranular slip at boundary irregularities of other types remains unexplored.

5.3. *Contributions of Different Dislocation Mechanisms to the Effect of Stimulation of Grain Boundary Sliding by Intragranular Slip*

In this section we describe dislocation mechanisms of different types of GBS observed experimentally and assess their contributions to the total amount of sliding. Let us consider pure GBS. This type of sliding can be described as the motion of glissile GBDs of

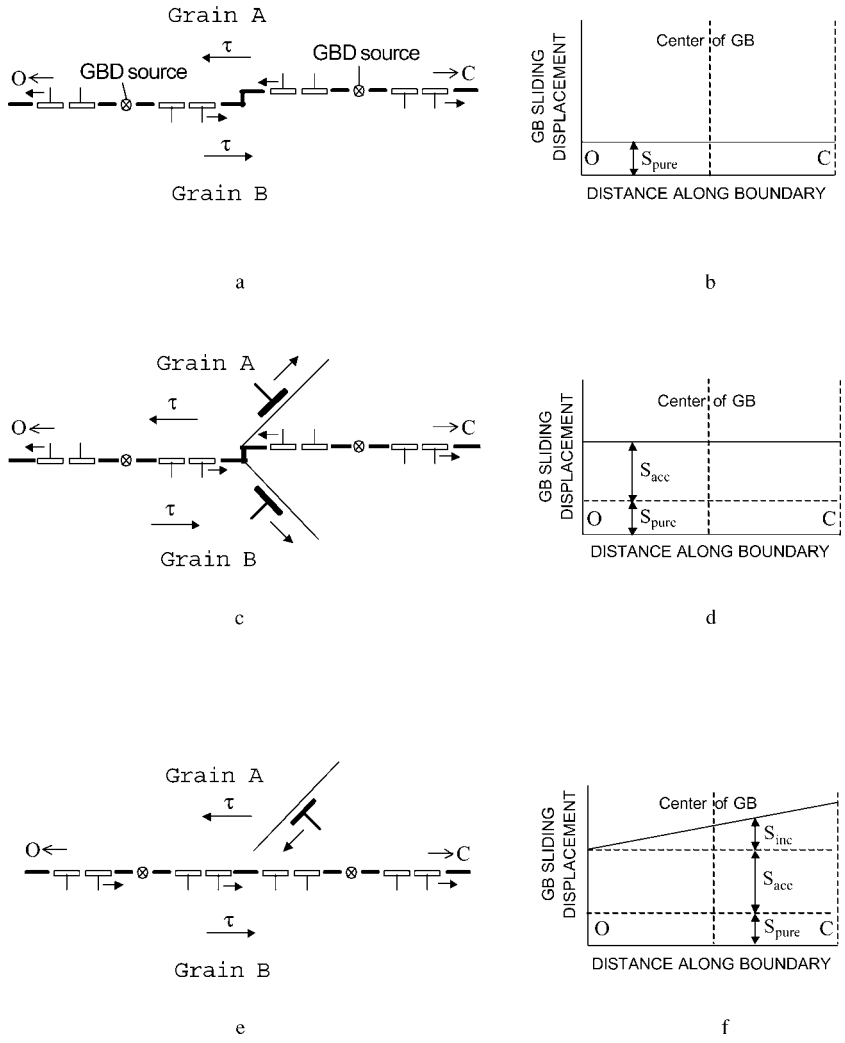

Figure 14. Dislocation models of different types of GBS (a, c, e), their interrelations and distributions along the boundary (b, d, f). Pure grain boundary sliding (a, b), sliding accommodated by slip (c, d) and superposition of the sliding accommodated by slip and GBS induced by incompatible deformation (e, f).

opposite signs generated by grain boundary sources (Fig. 14(a)). Under the effect of shear stress applied along the boundary these GBDs moves in opposite directions. Although the exact mechanism of their generation is unknown it is reasonable to suppose that the numbers of GBDs of opposite signs are similar. At macroscopic level the motion of these dislocations should result in a uniform distribution of the sliding along the boundary (Fig. 14(b)). However, real boundaries contain such irregularities as steps and facets. Therefore, spatial oscillations are typical for GBS. Actuation of slip during compatible deformation significantly enhances the sliding rate. As shown in previous section the accommodation of GBS by slip seems to be the most possible mechanism of stimulation of GBS (Fig. 14(c)). It is expected that in this case the amount of GBS remains uniformly distributed along the boundary (Fig. 14(d)). Incompatible deformation is characterized by the appearance of glissile GBDs of one sign whose interaction with glissile GBDs of opposite sign generated by grain boundary sources leaves GBDs of one sign (Fig. 14(e)). At respectively small intragranular strain rates and/or small component of intragranular shear along the boundary all these GBDs should move under the applied shear stress, i.e., their motion should occur in the direction of point C. Strong

elastic interaction between glissile GBDs with themselves can be avoided despite their motion are hindered by different boundary irregularities. Therefore, GBS at the boundary end O is produced purely by the operation of dislocation grain boundary sources. Motion of GBDs of one sign in one direction means that all these slip induced dislocations give a contribution to total sliding. At spatially uniform intragranular deformation the amount of sliding should increase linearly from point O to point C (Fig. 14(f)).

Let us assess contributions of different types of sliding on the basis of our experimental results. The total amount of sliding can be determined as

$$S_{\text{tot}} = S_{\text{pure}} + S_{\text{acc}} + S_{\text{inc}}, \tag{3}$$

where S_{pure}—amount of pure GBS, S_{acc}—amount of sliding is due to accommodation by slip, S_{inc}—amount of sliding induced by strain incompatibility. Contributions of different dislocation mechanisms to total effect of stimulation for different testing time are shown in Fig. 15. The assessment is made for the first 22 s of testing. Further deformation results in slide hardening followed by the negative sliding near point O. This means that amount of the boundary sliding in point O cannot be determined by the amount of the sliding accommodated by slip. It is seen that contribution of pure sliding reaches 40% at the beginning of deformation and then decreases by half. At the beginning of deformation the contribution of the effect of accommodation of GBS by slip to the total amount of the boundary sliding is 50%. Then it slightly decreases up to 40%. The maximum contribution of the sliding induced by strain incompatibility (determined near point C) increases from 10% at the beginning of deformation up to 40% before slide hardening. Thus, the effect of accommodation of the boundary sliding by crystallographic slip is significant and comparable with pure GBS only at the beginning of deformation. Further deformation makes the maximum effect of stimulation of GBS exerted by strain incompatibility as significant as the effect of accommodation of the sliding by intragranular slip.

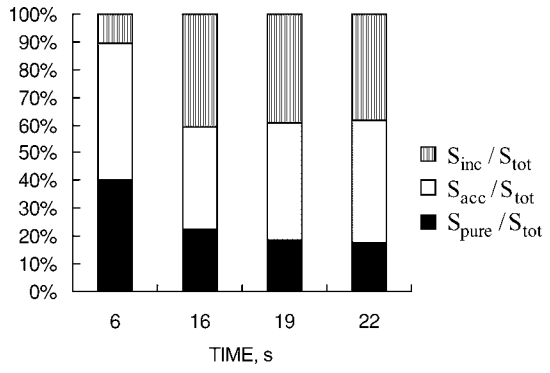

Figure 15. Contributions of different types of GBS to the total sliding determined from experimental data.

6. Summary

Experiments with zinc bicrystals have been designed to study the effect of intragranular slip on grain boundary sliding at originally compatible deformation taking into account possible dislocation reactions. For comparison, bicrystal of the same type has been tested at a slightly lower stress which is not enough to initiate intragranular slip. The results obtained show that actuation of intragranular slip results in the increase in the sliding rate more than five times in contrast to that without slip. Also, a good correlation between slip and GBS during deformation prior to slide hardening has been established. Slide hardening and negative grain boundary sliding near one end of the boundary are corresponded to the increased difference in strain rates in the neighboring grains. Assuming that the interaction between lattice dislocations and the boundary produces primarily glissile grain boundary dislocations of two opposite signs, an analysis of their contribution to GBS has been done. It has been shown that these grain boundary dislocations can induce only local GBS and cannot contribute to usual macroscopic grain boundary sliding. It has been proposed that close relationship between slip and GBS at compatible deformation is based on the accommodation of grain boundary sliding by crystallographic slip at grain boundary irregularities. It has been shown that grain boundary sliding is also stimulated by plastic strain incompatibility appearing in the course of the change in bicrystal geometry. These two different dislocation mechanisms can give almost the same contribution to the total amount of GBS accompanied by slip. The reasons for the suppression of grain boundary sliding can be both a non-smooth boundary and plastic strain incompatibility appearing with bicrystal straining.

Acknowledgments

This research was supported by NSF Grant DMR-0109535. The financial support of Fonds FCAR (Canada) is also gratefully acknowledged.

References

1. N.R. Adsit and J.O. Brittain, Trans. AIME **233**, 305 (1965).
2. O.A. Kaibyshev, V.V. Astanin, R.Z. Valiev, and V.G. Khairullin, Phys. Met. Metallogr. **51**, 166 (1981).
3. H. Fukutomi, H. Takatori, and R. Horiuchi, Trans. Japan Inst. Metals **23**, 579 (1982).
4. A.D. Sheikh-Ali, Scripta Metall. Mater. **33**, 795 (1995).
5. C.A.P. Horton, N.B.W. Thompson, and C.J. Beevers, Metal Sci. J. **2**, 19 (1968).
6. R.Z. Valiev and O.A. Kaibyshev, Physica Status Solidi (a) **44**, 477 (1977).
7. V.N. Perevezentsev, V.V. Rybin, and V.N. Chuvil'deev, Acta Metall. **40**, 887 (1992).
8. J. Weertman, J. Appl. Phys. **26**, 1213 (1956).
9. D. McLean, Philos. Mag. **23**, 467 (1971).
10. K. Reading and D.A. Smith, Philos. Mag. **A51**, 71 (1985).
11. R.Z. Valiev, V.G. Khairullin, and O.A. Kaibyshev, Fizika Metallov i Metallovedenie **63**, 396 (1987).
12. R.C. Gifkins, Scripta Met. **25**, 1397 (1991).
13. K. Xia, Mater. Sci. Forum **189/190**, 341 (1995).
14. G.R. Kegg, C.A.P. Horton, and J.M. Silcock, Philos. Mag. **A27**, 1041 (1973).
15. R.S. Gates, Acta Metall. **21**, 855 (1973).
16. R.C. Pond, D.A. Smith, and P.W.J. Southerden, Philos. Mag. **37**, 27 (1978).
17. S.E. Babcock and R.W. Balluffi, Acta Metall. **37**, 2357 (1989).
18. R.Z. Valiev, V. Yu. Gertsman, O.A. Kaibyshev, and Sh. Kh. Khannanov, Physica Status Solidi (a) **17**, 97 (1983).
19. A.D. Sheikh-Ali and J.A. Szpunar, Philos. Mag. Lett. **79**, 545 (1999).
20. J.D. Livingston and B. Chalmers, Acta Metall. **5**, 322 (1957).
21. J.J. Hauser and B. Chalmers, Acta Metall. **9**, 802 (1961).
22. J.P. Hirth, Metall. Trans. **3**, 3047 (1972).
23. E. Schmid and W. Boas, *Plasticity of Crystals with Special Reference to Metals* (Chapman and Hall, London, 1968), p. 59.
24. F. Garofalo, *Fundamentals of Creep and Creep-Rapture in Metals* (Macmillan, New York, 1965), p. 19.
25. A.D. Sheikh-Ali and R.Z. Valiev, Scripta Metall. Mater. **31**, 1705 (1994).
26. A.D. Sheikh-Ali and R.Z. Valiev, Scripta Metall. Mater. **32**, 1977 (1995).
27. A.D. Sheikh-Ali and J.A. Szpunar, Materials Science Forum **294–296**, 645 (1999).
28. A.P. Sutton and V. Vitek, Phil. Trans. R. Soc. **A309**, 1 (1983).
29. A.P. Sutton and R.W. Balluffi, *Interfaces in Crystalline Materials* (Clarendon Press, Oxford, 1995), p. 726.
30. A.D. Sheikh-Ali, Acta Mater. **45**, 3109 (1997).
31. A.D. Sheikh-Ali, F.F. Lavrentyev, and Yu.G. Kazarov, Acta Mater. **45**, 4505 (1997).
32. A. Jacques, A. George, and X. Baillin, in *Strength of Metals and Alloys (ICSMA 8)*, edited by P.O. Kettunen, T.K. Lepisto, and M.E. Lehtonen (Pergamon Press, Oxford, 1989), Vol. 1, p. 245.
33. A.I. Pshenichnyuk, V.V. Astanin, and O.A. Kaibyshev, Phil. Mag. **A77**, 1093 (1998).